Journal of Power Sources 197 (2012) 65–71

Contents lists available at SciVerse ScienceDirect

Journal of Power Sources

journal homepage: www.elsevier.com/locate/jpowsour

# Coulometric study of ethanol adsorption at a polycrystalline platinum electrode

Sol Gilman*

*Sensors and Electron Devices Directorate, U.S. Army Research Laboratory, 2800 Powder Mill Road, Adelphi, MD 20783-1197, United States*

ARTICLE INFO

*Article history:*
Received 7 July 2011
Received in revised form
16 September 2011
Accepted 17 September 2011
Available online 21 September 2011

*Keywords:*
DMFC
Ethanol
Ethanol fuel cells
Adsorption

ABSTRACT

For the first time, use of a novel pre-conditioning sequence and measurements of hydrogen blockage during fast cathodic scans has enabled the determination of rates of accumulation of ethanolic species on the surface of a platinum electrode under well-controlled conditions of surface cleanliness/activity and mass transport. For dilute solutions of ethanol in 1 N perchloric acid ($HClO_4$), oxidative adsorption rates maximize at 0.3 V, drop off at more cathodic potentials due to competition with adsorbed hydrogen and drop off at more anodic potentials due to oxidative processes that produce products released to the electrolyte. The time and concentration dependence of adsorption follows relationships that are common for adsorption on a heterogeneous surface. Some evidence are presented supporting a mechanism for production of soluble products that does not involve the adsorbed species that are detected through the measurement of blockage of hydrogen adsorption sites.

Published by Elsevier B.V.

## 1. Introduction

The anodic oxidation of ethanol has been a topic of considerable interest during the last decade in connection with the interest in using ethanol as an alternative to methanol in ambient temperature fuel cells (see, for instance, Ref. [1]). Adsorption processes can be expected to play a major role in the overall oxidation reaction. The adlayer on a platinum electrode in acid solution can be expected to contain a number of fragments of the original ethanol molecule that vary in composition with potential. In recent years, a number of in situ spectroscopic techniques have been applied to the issue of composition. This includes the identification in the adlayer of adsorbed carbon monoxide [2–9], adsorbed acetaldehyde and acetyl radicals [8–15], adsorbed acetate [16–19], and adsorbed methyl groups ($CH_x$) [20,21]. There is evidence for the existence of all of those species, besides acetate, at potentials below ~0.5 V and for adsorbed acetate at the higher potentials, the latter not expected to contribute to the results reported here. There is consensus [21–24] that the products that are desorbed and released to the electrolyte under a range of anodic conditions are mixtures of carbon dioxide, acetaldehyde, and acetic acid. One area not yet covered by previous investigators is the rate of accumulation of ethanol-derived species on the electrode surface and its relationship to the soluble product-producing anodic current. In this study, a "staircase" of pre-conditioning potentials and rapid potential scans were combined to provide information on the rate and extent of overall surface coverage in the early stages of ethanol adsorption under well-defined conditions of mass transport and surface preparation. It is anticipated that the approach could provide an additional tool for evaluation of other noble metals and noble metal alloys that can provide what amounts to an adsorbed oxygen "valve" for initiating adsorption/reaction on a clean and activated surface.

## 2. Experimental

### 2.1. Supplies and equipment

All measurements were made at room temperature (21 °C) in a 1 N solution of perchloric acid with various additions of ethanol. The acid solution was prepared using "Millipore" water with a resistivity of 18.2 MΩ cm and redistilled $HClO_4$ (Sigma–Aldrich). Ethanol was 99.5% American Chemical Society (ACS) reagent grade (Aldrich). The electrolyte solution was purified as described below, using a "getter" electrode. The getter electrode was cathodically/anodically cycled several times in an exterior solution. After the final anodic treatment (producing a protective passive state), the electrode was transferred to the test vessel, cathodically reduced, and held at 0.4 V for several hours with vigorous bubbling of argon. Electrochemical measurements were made using a Gamry Reference 3000 potentiostat. The electrochemical vessel was constructed of Pyrex glass with polytetrafluoroethylene (PTFE) stoppers and a PTFE tube for degassing the solution with reagent grade argon.

### 2.2. Electrodes

The working electrode was a commercially pure (CP) grade platinum wire of 0.08 cm in diameter and 1 cm in length. The wire was

* Tel.: +1 301 394 0339.
*E-mail address:* sol.gilman.civ@mail.mil

0378-7753/$ – see front matter. Published by Elsevier B.V.
doi:10.1016/j.jpowsour.2011.09.041

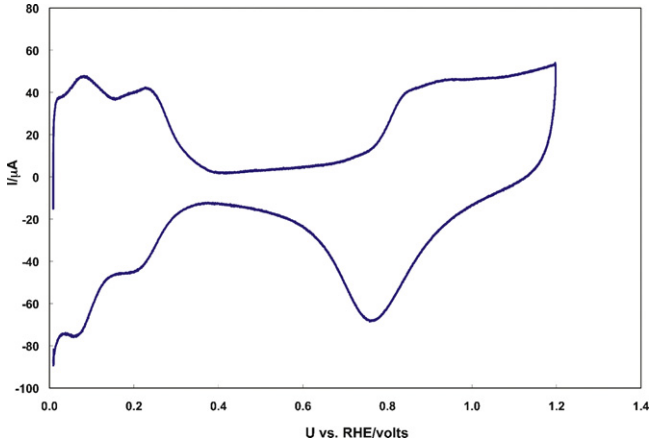


**Fig. 1.** Voltage scan for a 1 N solution of $HClO_4$, sweep speed, $\nu = 100\,mV\,s^{-1}$.

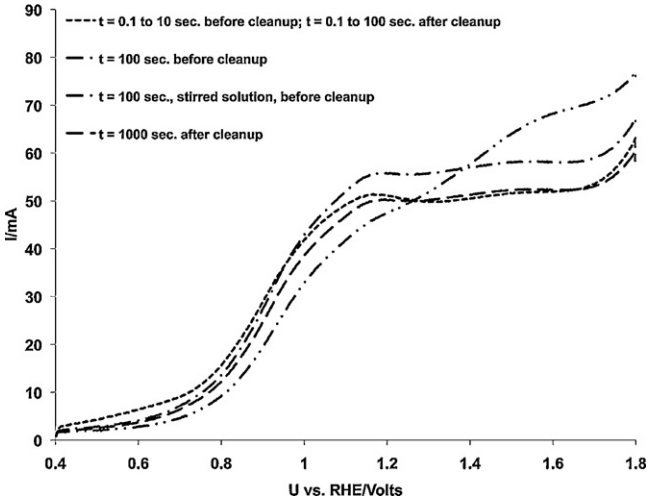


**Fig. 3.** Anodic scans for 1 N $HClO_4$ using the sequence in Table 1, $\nu = 200\,V\,s^{-1}$.

etched lightly in aqua regia, flame annealed, encased in shrinkable PTFE tubing to expose a 1-cm length, and then lightly etched again. The working electrode was periodically immersed in a hot chromic acid cleaning solution. Based on cathodic hydrogen adsorption [25], the electrode had a roughness factor of 2.1 that remained constant over several months of use. The counter electrode was a platinized platinum (Pt) foil with a 2-$cm^2$ geometric area. The use of a palladium/hydrogen (Pd/H) electrode as reference allowed very close placement parallel to the working electrode. It was prepared in a manner similar to that described by Fleischmann and Hiddleston [26]: a 0.076-cm-diameter wire with a length of 1 cm was spot-welded to a long Pt wire that was sealed in a shrinkable PTFE tube so as to conceal the weld. The electrode was etched in aqua regia and made cathodic at 24 mA for 17 min (past the point of coulombic stoichiometry for PdH) and then anodic for 4.5 min. This electrode was found to be stable for several days with a potential of approximately 0.02 V versus a reversible hydrogen electrode. The electrode was re-hydrogenated daily and its potential was monitored against a saturated calomel electrode (SCE) every few hours. All potentials applied and reported here were adjusted to that of a reversible hydrogen electrode. The "gettering" electrode used for electrolyte purification was a platinized Pt gauze cylinder, 55 mm long and 15 mm in diameter.

### 2.3. Procedures

#### 2.3.1. Cyclic voltammograms

Two voltammograms are shown in Figs. 1 and 2 for the purpose of explaining the pulse sequences used to obtain the adsorption data discussed in the sections that follow. Fig. 1 is the familiar trace obtained for the electrolyte (1 N $HClO_4$) used throughout this investigation. The "hydrogen adsorption" region extends from ~0 to 0.3 V and is symmetrical. Fast cathodic scans in that region were used to obtain the adsorption data reported below. The "oxygen adsorption" region begins at ~0.8 V and continues until the current increases exponentially corresponding to oxygen evolution. Fast anodic scans were used to obtain the information on electrolyte purity described below. "Oxygen" adsorption is not symmetrical, but occurs with a negative peak below ~0.8 V. In the electrode pre-conditioning sequences, advantage was taken of the passivity of the electrode in the vicinity of 1.2 V after anodization at 1.8 V. Fig. 2 is a similar voltammogram obtained after making the electrolyte $10^{-3}$ M in ethanol. On this scale, the oxygen and hydrogen adsorptions are not visible, because the corresponding currents are extremely small compared to those shown that correspond to ethanol oxidation that results in soluble products released to the electrolyte (as opposed to adsorbed species). The trace shows that an electrode exposed to high potentials becomes passive until reduced at potentials below ~0.8 V. The region of passivity was used in preparing a clean surface in the adsorption studies discussed below.

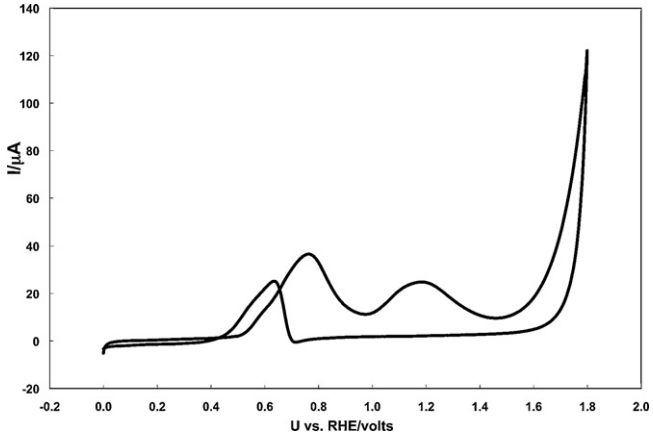


**Fig. 2.** Cyclic voltammogram for $10^{-3}$ M ethanol in 1 N $HClO_4$, $\nu = 1\,mV\,s^{-1}$.

#### 2.3.2. Anodic scans

Anodic scans can provide a sensitive test for purity of the baseline electrolyte or a measure of amount of adsorbed organic material. A sequence of potential steps was used to clean the electrode surface and follow adsorption from essentially 0 time with respect to transport of material from the solution. The potential sequence used and the rationale for the various steps of the sequence appears in Table 1. A similar approach has been used in the past to study the adsorption of CO and other organic molecules (see, for instance, Ref. [27]). Some resulting scans appear in Figs. 3 and 4.

Slow anodic scans using the preconditioning steps in Table 1 were used to obtain "polarization" curves for a number of methanol concentrations. The scans appear in Fig. 5.

#### 2.3.3. Cathodic scans

Cathodic scans can be used to measure hydrogen adsorption sites that are obscured by an adsorbate. The potential sequence used and the rationale for each step appears in Table 2. All steps after #3 are in the quiescent solution. Some representative scans appear in Fig. 6.

**Table 1**
Sequence used for anodic scans.

| Step # | Potential (V) | Conditions | Purpose |
|---|---|---|---|
| 1 | 0.0 | Bubble/stir with argon for 1 s | Desorb anionic impurities |
| 2 | 1.8 | Bubble/stir with argon for 1 s | Oxidize organics & passivate surface |
| 3 | 1.2 | Bubble/stir with argon for 30 s; quiescent for 90 s | Degas solution/retain passivity |
| 4 | 0.4 | Quiescent solution for specified adsorption time | Reduction of passive surface within first few milliseconds; begin adsorption with no depletion of diffusion layer |
| 5 | Anodic scan at 200 V $s^{-1}$ | Quiescent solution | Detect adsorbed material |
| 5 (alternative) | Anodic scan at 1 mV $s^{-1}$ | Quiescent solution | Measure "polarization curve" |

**Table 2**
Sequence used for cathodic scans.

| Step # | Potential (V) | Conditions | Purpose |
|---|---|---|---|
| 1–3 | Same as Table 1 | Same as Table 1 | Same as Table 1 |
| 4 | 0.1 | 0.01 s pulse | Rapid reduction of surface |
| 5 | 0.4 | 0.01 s pulse | Rapid removal of adsorbed H |
| 6 | Variable voltage or open circuit | Variable time adsorption time, *t* | Allow adsorption under controlled conditions of surface & transport |
| 7 | 0.4 V | 0.01 s pulse | Provide same starting potential for scans |
| 8 | Cathodic scans | Variable sweep speeds | Measurement of hydrogen adsorption sites not obscured by other adsorbates |

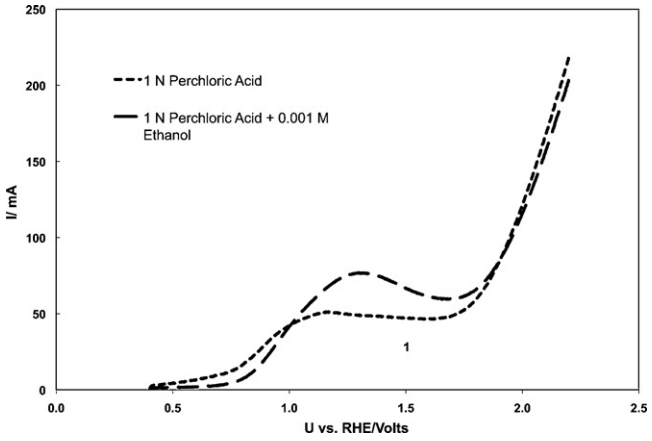


**Fig. 4.** Anodic scans with/without ethanol addition, using the sequence in Table 1, $v = 200$ V $s^{-1}$.

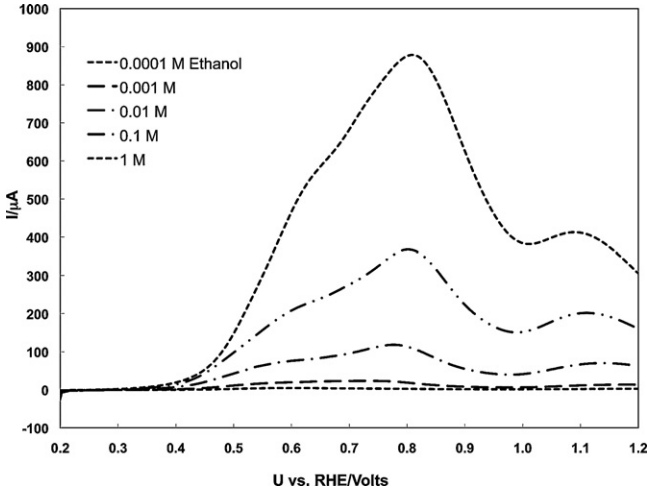


**Fig. 5.** Polarization curves for ethanol oxidation/desorption using the sequence in Table 1, $v = 1$ mV $s^{-1}$.

## 3. Results and discussion

### 3.1. Electrolyte purity

Anodic scans, such as those displayed in Fig. 3 (using the sequence in Table 1), provide a sensitive indication of solution purity before and after purification using a "gettering" electrode. Although high purity $HClO_4$ and high resistivity "Millipore" water were used for preparing the electrolyte, anodic scans similar to the first trace in the figure were obtained when the exposure time was less than ~10 s and longer than ~100 s after purification. Before purification very significant changes in the scan were observed at exposure times longer than ~10 s (second and third traces). That the effect becomes more rapid with stirring indicates that the adsorption of impurities is at least partially diffusion-controlled. In view of the high resistivity of the water, it seems likely that the impurities are neutral organic molecules exuded from the Millipore membranes. "Gettering" of the electrolyte for several hours was found to result in scans that overlapped for adsorption times of from 0.1 to 100 s. The result at 1000 s (fourth trace) shows some distortion of the scan. All of the ethanol adsorption data discussed below were obtained after "gettering" the electrolyte for 3 h.

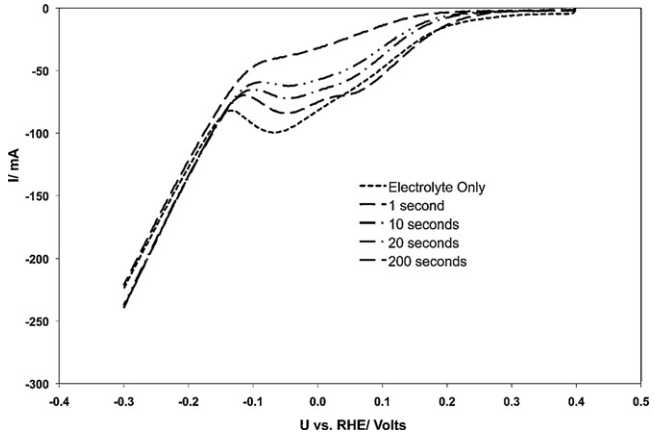


**Fig. 6.** Representative cathodic scans at $v = 200$ V $s^{-1}$ for adsorption of ethanol from a $10^{-3}$ M solution of ethanol in 1 N $HClO_4$.

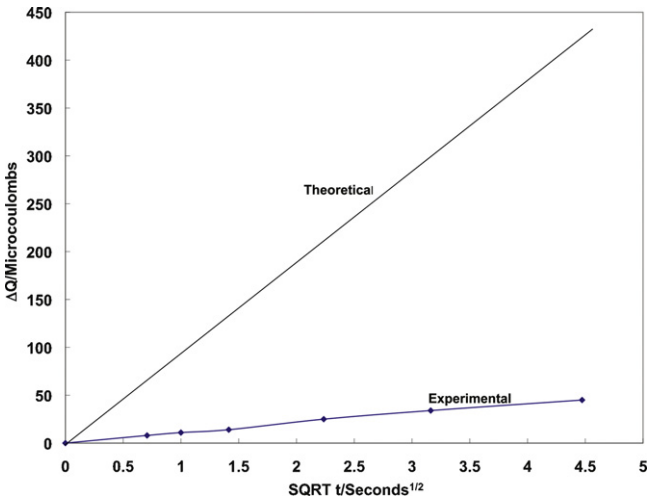


**Fig. 7.** Comparison of experimental $\Delta Q$ (decreased hydrogen adsorption charge) corresponding to ethanol adsorption ($10^{-3}$ M solution at 0.3 V) with calculated $\Delta Q$ assuming one hydrogen adsorption site/ethanol molecule adsorbed.

### 3.2. Adsorption measurements using anodic scans

An attempt was made to follow the adsorption of ethanol using the anodic scan sequence in Table 1. The adsorption time and ethanol concentration for the representative scans in Fig. 4 correspond to a fractional surface coverage of 0.54 as determined by the cathodic scan approach discussed below. If the anodic scans were a reliable measure of surface coverage, one would expect the two curves in Fig. 4 to merge at the highest potentials of the scans. The fact that they do not implies that they do not represent the same state of the surface (incomplete oxidation/desorption of the organic adlayer). Also, the differential areas between the two curves (providing coulombs corresponding to oxidation of the adlayer) were found to vary significantly with sweep speed. Finally, information is not available on the final desorbed product under fast-scan conditions. As mentioned previously, long-term oxidation has been reported to result in a mixture of acetaldehyde, acetic acid, and carbon dioxide. In view of these complexities, the use of anodic scans in this study was abandoned.

### 3.3. Adsorption measurements using cathodic scans

#### 3.3.1. Reproducibility and significance of cathodic coulombic measurements

Using the sequence in Table 1, cathodic scans for the same electrode such as those that appear in Fig. 6 were found to be extremely reproducible using purified electrolyte, allowing overlap of traces over a period of months of experimentation. With the addition of ethanol, estimates of coulombic charge were reproducible to within several percent. The coulombs of charge expended during a cathodic scan into the "hydrogen adsorption" region (before exponential increase of current corresponding to hydrogen gas evolution) of a Pt electrode is generally accepted to correspond mainly to deposition of a monolayer of hydrogen atoms [28]. Integration of the coulombic area (with the *x*-axis scale converted to seconds) of the trace 1 for the electrolyte in Fig. 6 provides the quantity $Q_H^{S*}$ that includes $Q_H^S$, the charge corresponding to monolayer hydrogen adsorption. Adsorption of organic species causes hydrogen adsorption sites to be blocked and similar integrations of traces 2–5 of the figure provide values of $Q_H^*$ that include values of $Q_H$, corresponding to adsorption of hydrogen on the partially blocked surface. In addition to $Q_H^S$ and $Q_H$ uncertainties involved in choosing the inflection point for the onset of hydrogen evolution. In this study, we are interested in the ratio: $(Q_H^S - Q_H)/Q_H^S$ to provide the fractional surface coverage, $\Theta$ corresponding to blockage of hydrogen adsorption sites and equivalently, the fractional surface coverage with ethanol-derived species. For that ratio, the extraneous charges of the corresponding starred quantities are expected largely to cancel out and provide a good approximation of $\Theta$. Another possible source of error is the desorption of ethanol during cathodic sweeps. Adsorbed ethanol does desorb at low potentials but at relatively slow rates as is discussed below. Values of $Q_H^*$ were obtained for sweep speeds from 100 to 1000 V after the electrode was loaded with 0.5 monolayer of ethanol. The values were found to be constant to within a few percent. That serves as one indication of the stability of the adlayer under the conditions of measurement of $\Theta$.

The rates of adsorption obtained in this study appear activation rather than diffusion controlled as indicated by the analysis that follows. Assuming diffusion control, mass transport in the early few seconds of adsorption would be expected to follow the following current–time relationship for semi-infinite linear diffusion [28]:

$$I_d = n\pi^{-1/2}FAD^{1/2}C\tau^{-1/2}. \quad (1)$$

Integrating Eq. (1), the corresponding charge is given by Eq. (2)

$$Q_d = 2nA\pi^{-1/2}FD^{1/2}Ct^{1/2}, \quad (2)$$

where

$n$ = number of electrons;
$F$ = Faraday constant;
$A$ = area = 0.26 $cm^2$; and
$D$ = diffusion coefficient of ethanol = $1.24 \times 10^{-5}$ $cm^2$ $s^{-1}$.

In Fig. 7, a plot of $Q_d$ ($n = 1$) of Eq. (2) is compared with $(Q_H^{S*} - Q_H^*) = \Delta Q$ obtained experimentally for adsorption from $10^{-3}$ M ethanol. Taking $n = 1$ is equivalent to the assumption that one molecule of ethanol blocks one hydrogen site. It can be seen from the comparison that diffusion control begins to exceed the adsorption results by over an order of magnitude at an early stage in the adsorption process. Also, $n$, and therefore $Q_d$, is likely to be larger than 1 (i.e., more than one hydrogen adsorption site blocked by ethanol fragments from one molecule of ethanol). Finally, some sample measurements of adsorption showed no influence of stirring.

#### 3.3.2. Rates of adsorption from a $10^{-3}$ M ethanol solution in 1 N $HClO_4$

Values of $\Theta$ versus time obtained at a sweep speed of 200 V $s^{-1}$ are plotted on a logarithmic scale in Fig. 8. Rates of adsorption, $d\Theta/dt$, can be derived from the semilog plot:

$$\frac{d\Theta}{d\ \log\ t} = \frac{t\,d\Theta}{dt}, \quad (3)$$

$$\frac{d\Theta}{dt} = \frac{(d\Theta/d\ \log\ t)}{t}. \quad (4)$$

No adsorption was evidenced at open circuit when small oxidative currents due to residual oxygen were avoided. That and the fact that adsorption is much diminished at the low potentials at which potential the surface is normally largely covered with adsorbed hydrogen supports Heinen et al.'s [8] conclusion that the first step in the adsorption process occurs with the abstraction of a hydrogen atom from the hydroxyl carbon. However, slight adsorption appears to persist to a potential as low as 0.02 V. Decreased adsorption at potentials above 0.5 V is readily attributable to the "steady" oxidation that is apparent from Fig. 5. Adsorption is maximal at 0.32 V, where there is little competition from hydrogen adsorption and oxidation/desorption (the latter according to the polarization curves in Fig. 5). Adsorption at 0.43 V is somewhat

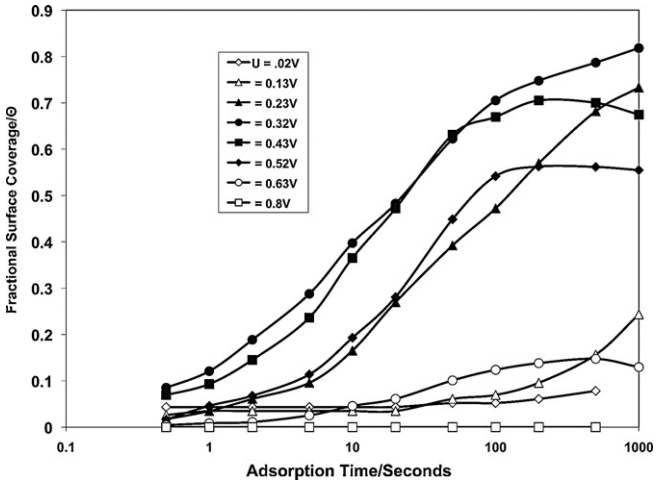


**Fig. 8.** Adsorption of ethanol from a $10^{-3}$ M solution in 1 N $HClO_4$.

reduced compared to 0.32 V in line with the observation of incipient "steady" oxidation at the higher potential according to Fig. 5. Because adsorption at 0.32 V is maximized, additional attention was paid to adsorption at that potential. It must be kept in mind that although 0.32 V is in a sense, a "neutral potential" for ethanol, the adsorbed molecule is not intact and the chemical composition is quite complicated according to the published results already mentioned above.

### 3.3.3. Concentration dependence of ethanol adsorption

Adsorption at 0.3 V for a number of different ethanol concentrations was measured and the plots appear in Fig. 9. Parallel linear regions can be seen in the mid-range of surface coverages for the different concentrations. This semi logarithmic dependence of surface coverage on adsorption time in the mid-range of surface coverages suggests adherence to the Elovich equation as is commonly encountered in gas phase kinetics on heterogeneous surfaces [29]:

$$\frac{d\Theta}{dt} = kCe^{-m\theta}. \tag{5}$$

Integrating and taking logarithms yields

$$\Theta = \ln kC(t - t_0). \tag{6}$$

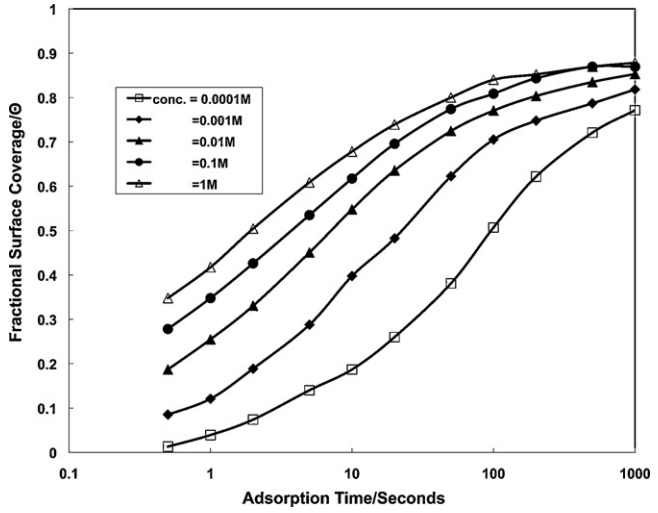


**Fig. 9.** Adsorption of ethanol at 0.3 V.

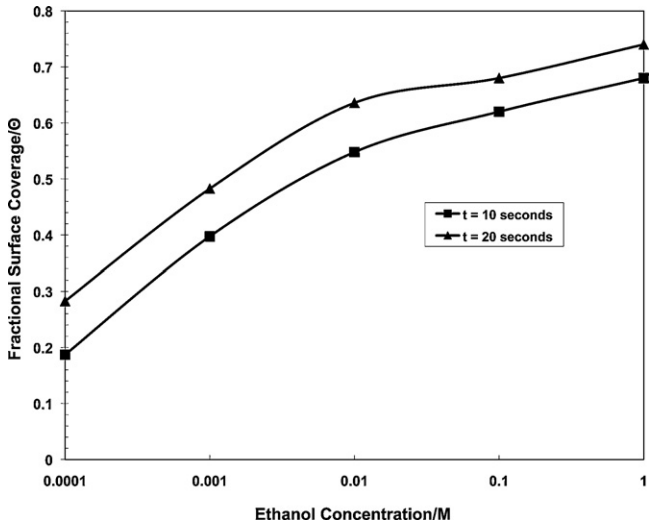


**Fig. 10.** Fractional surface coverage with ethanol at fixed adsorption time.

It should be noted that for the parallel regions of the plots the rates of adsorption in that range are the same for the same elapsed time but differ for the same fractional coverage according to their elapsed times (see Eq. (4)). It is apparent from Fig. 9 that adsorption rates do not have a linear dependence on concentration. For the range of $\Theta$ where Eqs. (5) and (6) apply, Eq. (6) predicts that $\Theta$ at constant adsorption time will depend linearly on the logarithm of concentration. Such plots appear in Fig. 10. The plots have fair linearity in the lower range of fractional coverages.

It is often observed that the adsorption rates on a heterogeneous surface follow a simple Langmuir relationship at low surface coverages (Fig. 11):

$$\frac{d\Theta}{dt} = k'C(1 - \Theta). \tag{7}$$

Rearranging Eq. (7) and integration of both sides of the equation yields

$$\ln(1 - \Theta) = k'Ct_0 - k'Ct, \tag{8}$$

where $t_0 = 0$.

Values of $\Theta$ were obtained for short adsorption times at 0.3 V using the sequence in Table 2 with $\nu = 1000\,\mathrm{V\,s^{-1}}$. Plots of $\ln(1 - \Theta)$ versus time for two different ethanol concentrations appear in Fig. 11. Regions of fair linearity are observed.

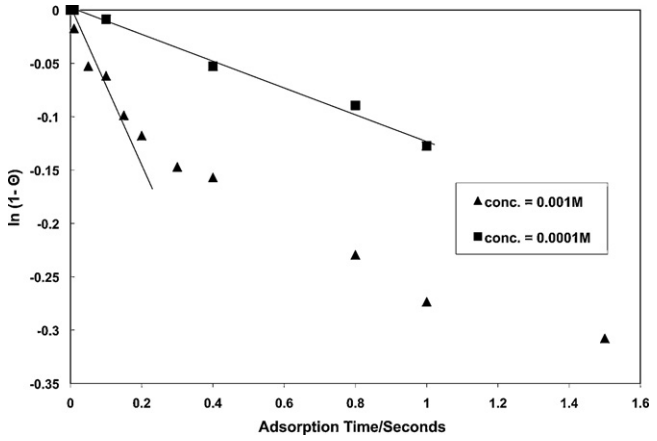


**Fig. 11.** Test of Eq. (8) for short adsorption times.

**Table 3**
Correlation of anodic current at 0.5 V to fractional surface coverage.

| Conc. ($M l^{-1}$) | $\Theta$ | $I_{an}$ (μA) | $I_{calc}$ (μA) | $I_{an}/I_{calc}$ |
|---|---|---|---|---|
| 0.0001 | 0.3 | 3.1 | 0.47 | 6.6 |
| 0.001 | 0.56 | 9.4 | 0.48 | 20 |
| 0.01 | 0.67 | 34.7 | 0.47 | 80 |
| 0.1 | 0.74 | 93 | 0.31 | 300 |
| 1 | 0.78 | 163 | 0.19 | 858 |

### 3.3.4. Desorption of adsorbed ethanol

Adsorbed ethanol can be desorbed to some extent at either cathodic or anodic potentials. The data plotted in Fig. 12 were obtained using the sequence in Table 2 with an additional potential step added after step 6 of that sequence. Ethanol was pre-adsorbed at 0.32 V and the desorption at 0.02 V were followed by applying cathodic scans. In the time allowed for the experiments, desorptions at 0.02 V did not go down to the same level as adsorption at the latter potential. According to Wang et al. [12] desorption products include methane and ethane suggesting that the desorbed species include the $CH_x$ species already mentioned in Section 1 above and other possibilities excluding adsorbed CO which is reportedly [2–9] the main non-desorbable component of the adlayer at the lower potentials. These results tend to confirm that there is no significant loss of charge during the cathodic scan experiments conducted at sweep speeds of 200 V $s^{-1}$ which involve exposure to low potentials for only a few milliseconds.

### 3.3.5. Correlation between adsorption rates and oxidation/desorption current

The observation of 0 coverage at 0.8 V in Fig. 8 can be ascribed to either the opposing rate of oxidation to soluble products (which reaches a maximum at that potential according to Fig. 5) or the onset of surface passivation by oxygen adsorption, that process beginning somewhat below that potential (see Fig. 1) or both. As oxygen adsorption is small at that potential, the former effect is likely to predominate at 0.8 V. The drop-off of anodic current above 0.8 V is probably due to the beginning of the passivation effect. The potential of 0.5 V is well into the first Tafel region [1] of the polarization curve and that region is of most relevance to fuel cell technology. An attempt was made to correlate the anodic currents measured at 0.5 V to the adsorption data in Fig. 9. This assumes that the adsorption rates measured at ~0.3 V represent maximal rates undiminished by rates of oxidation or cathodic desorption. Table 3 lists values of $\Theta$ after 200 s of adsorption at 0.5 V (maximal adsorption at that potential) and the corresponding anodic currents $I_{an}$ obtained just before measurement of $\Theta$ (step 6 in Table 2). Values of $I_{calc}$ were calculated using the data in Fig. 9 to provide monolayers/second and by multiplying those values by 115 microamperes/monolayer of hydrogen for this electrode. $I_{calc}$ is the current equivalent to hydrogen site occupation using Eq. (9):

$$I_{calc} = 115\left(\frac{d\Theta}{dt}\right). \tag{9}$$

If the anodic current were limited by the measured rate of adsorption, there would be a number of possibilities for the value of the ratio $I_{an}/I_{calc}$:

1. The minimal ratio would be 1, corresponding to a one-electron oxidation of one-site attached $CH_3CH_2O$ surface species to acetaldehyde.
2. The maximal ratio could be as high as 11, corresponding to oxidation of a one-site attached $CH_3CH_2O$ surface species to carbon dioxide and protons.
3. Ratios between 1 and 11 could correspond to the oxidation of a mixture of $CH_3CH_2O$ and adsorbed ethanol fragments to carbon dioxide or other products.

For most of the concentrations listed in Table 3, $I_{an}/I_{calc}$ is much higher than 11 (possibility 2). Hence, only a small fraction of the anodic current, $I_{an}$ at the higher concentrations must be used in reducing $\Theta$ from the corresponding larger value predicted by the adsorption rates at 0.3 V to the lower values listed in Table 3. A possible mechanism that could support the higher fraction of $I_{an}$ is the oxidation of ethanol on bare Pt surface sites (zero concentration of adsorbed intermediate). It is also noteworthy that $I_{calc}$ remains fairly constant over a wide range of concentrations. That may imply that the fraction of adsorbed material that does act as an intermediate for a smaller fraction of the total current, remains constant over a corresponding wide range of bulk ethanol concentrations. Thus, $I_{an}$ would have two components:

$$I_{an} = I_{ads} + I_b, \tag{10}$$

where $I_{ads}$ and $I_b$ are the fractions of the total anodic current that proceeds on surface sites covered with an oxidation intermediate and bare surface sites, respectively. From the analysis of Table 3, $I_{ads}$ remains fairly constant with increasing bulk concentration of ethanol, whereas $I_b$ rises steadily with increasing ethanol concentration. This seems to correlate well with the spectroscopic evidence presented by Camara and Iwasita [30], who concluded that oxidation of ethanol at 0.5 V proceeds by two different mechanisms: one that produces low yields of acetic acid and carbon dioxide and is relatively concentration insensitive, and the other that produces relatively high yields of acetaldehyde as the bulk concentration of ethanol is increased. Because oxidation of ethanol to acetaldehyde requires no addition of oxygen (from water), it is plausible that this could occur on isolated bare or high-turnover surface sites. On the other hand, oxidation to acetic acid and carbon dioxide would likely involve a two-site adsorption, one-site providing "adsorbed water," or more specifically, a hydroxyl radical.

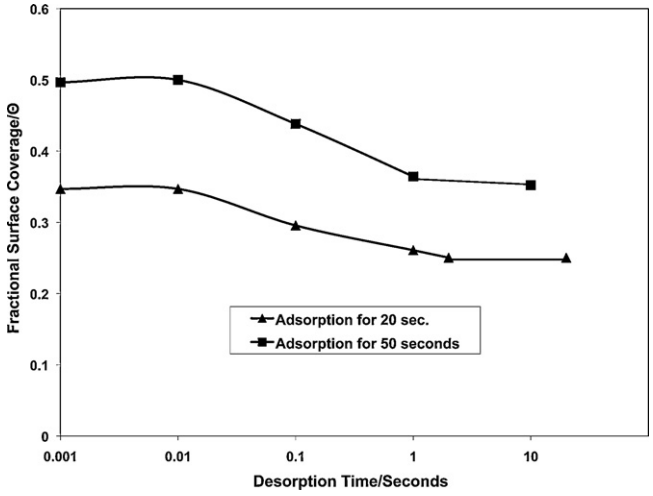


**Fig. 12.** Desorption of ethanol at 0.02 V after adsorption at 0.32 V.

## 4. Conclusions

The surface conditioning and electrolyte purification procedures used in this study allowed monitoring of a single adsorption event for upwards of 1000 s under well-defined conditions of surface cleanliness and mass transport conditions. The adsorption of

ethanol from dilute solutions in 1 N $HClO_4$ was studied by coulometric measurement of the hydrogen adsorption sites blocked by the adsorbed organic material. The rate of adsorption and saturation coverage is maximal at ~0.3 V. That potential is in the "double layer region" (i.e., free of adsorbed hydrogen and oxygen from the electrolyte) and at that potential there is no significant oxidation of ethanol that releases products from the surface to the electrolyte. The adsorption does not occur at open circuit and drops off at more cathodic potentials consistent with the conclusion by Heinen et al. [8] that the first step in the adsorption process is removal of a proton. The rates of adsorption at 0.3 V over a wide range of ethanol concentrations exhibits a logarithmic dependence on adsorption time as is common for a heterogeneous surface (Elovich relationship). That leads to the conclusion that the adsorption at ~0.3 V is a relatively slow surface chemical process that follows the relatively rapid abstraction of a hydrogen atom. Rates of adsorption drop off steeply at potentials higher than ~0.4 V, where ethanol is oxidized to soluble products. Similar time-dependencies of adsorption were reported for a number of organic molecules including butanol by Bockris and Jeng [31]. An attempt to correlate the "steady" oxidation currents at 0.5 V to the maximal adsorption rates measured at 0.3 V leads to the conclusion that the latter currents do not derive wholly from the adsorbed intermediates measured in this study, which is consistent with a mechanism of "parallel pathways" for ethanol oxidation as proposed by Camara and Iwasita [30].

## Acknowledgements

The author is grateful to Drs. Edward Shaffer and Cindy Lundgren for generous support of this project. Thanks to Dr. Jeffrey Read and to Michelle Marx for helpful discussions and assistance in establishing the experimental instrumentation.

## References

[1] L. Jiang, A. Hsu, D. Chu, R. Chen, Int. J. Hydrogen Energy 35 (2010) 365–372.
[2] L.-W.H. Leung, S.C. Chang, M.J. Weaver, J. Electroanal. Chem. 266 (1989) 317.
[3] S.C. Chang, L.-W.H. Leung, M.J. Weaver, J. Phys. Chem. 9 (1990) 6013.
[4] J.L. Rodríguez, E. Pastor, X.H. Xia, T. Iwasita, Langmuir 16 (2000) 5479.
[5] J.F. Gomes, B. Busson, A. Tadjeddine, J. Phys. Chem. B 110 (2006) 5508.
[6] A. Lagutchev, G.Q. Lu, T. Takeshita, D.D. Dlott, A. Wieckowski, J. Chem. Phys. 125 (2006) 154705.
[7] J.F. Gomes, B. Busson, A. Tadjeddine, G. Tremiliosi-Filho, Electrochim. Acta 53 (2008) 6899.
[8] M. Heinen, Z. Jusys, R.J. Behm, J. Phys. Chem. C 114 (2010) 9850–9864.
[9] B. Kutz, R. Björn, B. Braunschweig, Mukherjee, L. Rachel, R.L. Behrens, D.D. Dlott, A. Wieckowski, J. Catal. 278 (2011) 181–188.
[10] B. Bittins-Cattaneo, S. Wilhelm, E. Cattaneo, H.W. Buschmann, W. Vielstich, Ber. Bunsen-Ges. Phys. Chem 92 (1988) 1210.
[11] N. Fujiwara, K.A. Friedrich, U. Stimming, J. Electroanal. Chem. 472 (1999) 120.
[12] H. Wang, C. Jusys, R. Behm, J. Fuel Cells 4 (2004) 113.
[13] C. Lamy, E.M. Belgsir, J.-M. Léger, J. Appl. Electrochem. 31 (2001) 799.
[14] T. Iwasita, J. Braz. Chem. Soc. 13 (2002) 401.
[15] M.H. Shao, R.R. Adzic, Electrochim. Acta 50 (2005) 2415.
[16] J. Shin, W.J. Tornquist, C. Korzeniewski, C.S. Hoaglund, Surf. Sci. 364 (1996) 122.
[17] X.H. Xia, H.-D. Liess, T. Iwasita, J. Electroanal. Chem. 437 (1997) 233.
[18] F. Colmati, G. Tremiliosi-Filho, E.R. Gonzalez, A. Berna, E. Herrero, J.M. Feliu, Faraday Discuss. 140 (2008) 379.
[19] V. Del Colle, A. Berna, G. Tremiliosi-Filho, E. Herrero, J.M. Feliu, Phys. Chem. Chem. Phys. 10 (2008) 3766.
[20] S.C.S. Lai, S.E.F. Kleyn, V. Rosca, M.T.M. Koper, J. Phys. Chem. *C* 112 (2008) 19080.
[21] H. Hitmi, E.M. Belgsir, J.M. Leger, C. Lamy, R.O. Lezna, Electrochim. Acta 39 (1994) 407.
[22] R. Ianniello, V. Sobkowski, J.L. Rodriguez, E. Pastor, J. Electroanal. Chem. 471 (1999) 167.
[23] F. Vigier, C. Coutanceau, F. Hahn, E.M. Belgsir, C.J. Lamy, J. Electroanal. Chem. 563 (2004) 81.
[24] F. Vigier, C. Coutanceau, A. Perrard, E.M. Belgsir, C. Lamy, J. Appl. Electrochem. 34 (2004) 439.
[25] F.G. Will, C.A. Knorr, Z. Electrochem. 64 (1960) 258.
[26] M. Fleischmann, J.N. Hiddleston, J. Phys. E Sci. Instrum. I (1968) 2.
[27] S. Gilman, J. Phys. Chem. 67 (1963) 78.
[28] New Instrumental Methods in Electrochemistry, Interscience Publishers, Inc., New York, NY, 1959, p. 62.
[29] Physical Chemistry of Surfaces, 3rd edition, John Wiley and Sons Inc., New York, 1976, p. 650.
[30] G.A. Camara, T. Iwasita, J. Electroanal. Chem. 578 (2005) 315–321.
[31] I.M. Bockris, K.T. Jeng, J. Electroanal. Chem. 330 (1992) 541.